

Original Article

Evaluation of hepatic fibrosis by using stretched-exponential and mono-exponential diffusion-weighted MR imaging

Fangfang Fu¹, Dapeng Shi¹, Shaocheng Zhu¹, Meiyun Wang¹, Cuiyun Chen¹, Dujuan Li², Jing Li¹, Shewei Dou¹

Departments of ¹Radiology, ²Pathology, The People's Hospital of Zhengzhou University & Henan Provincial People's Hospital, Zhengzhou 450003, Henan, China

Received June 3, 2016; Accepted August 8, 2016; Epub November 15, 2016; Published November 30, 2016

Abstract: Aim: To obtain the parameters from stretched-exponential and mono-exponential models of multiple b-value diffusion weighted imaging (DWI) and to compare the value of these parameters in detecting and staging hepatic fibrosis (HF). Methods: The apparent diffusion coefficient (ADCst), distributed diffusion coefficient (DDC) and intravoxel water diffusion heterogeneity (α) for the study and control groups were calculated and compared. T-test, Receiver Operating Characteristic (ROC) analysis and Pearson's correlation coefficient were used for statistical analysis. Results: All the parameters in the study group were significantly different from the corresponding parameters in the control group ($P < 0.05$). The DDC showed a strong negative correlation with the HF stages ($r = -0.786$, $P < 0.001$). The ADCst showed a moderate negative correlation with the HF stages ($r = -0.579$, $P < 0.001$). However, α showed no correlation with the HF stages ($P > 0.05$). The α also showed no obvious differences when comparing fibrosis at different stages. Using ROC analysis, DDC showed greater capability than ADCst in discriminating fibrosis stage 1 or greater ($\geq F1$), stage 2 or greater ($\geq F2$), and stage 3 or greater ($\geq F3$), the areas of under curve (AUCs) of DDC and ADCst were 0.948, 0.903, 0.879, 0.912, 0.850 and 0.741, respectively. There was a moderate positive correlation between ADCst and DDC ($r = 0.596$, $P < 0.001$). Conclusions: DDC and ADCst showed a significant correlation with the stages of HF. The DDC had higher predictive ability than ADCst in distinguishing the stages of HF.

Keywords: Hepatic fibrosis, diffusion weighted imaging, mono-exponential diffusion, stretched-exponential diffusion

Introduction

Chronic liver diseases could cause hepatic fibrosis (HF) [1, 2]. The progression of HF might eventually cause hepatic cirrhosis, hepatocellular carcinoma, and even hepatic failure [3-5]. Early diagnosis and classification of HF is critical, because it could help determine early treatments, prevent its progression to hepatic cirrhosis, and reduce healthcare costs [1, 6, 7]. In the clinic, it is difficult to diagnose and stage HF because patients with chronic liver diseases usually have no symptoms or only show slight abdominal distension. To date, the result of liver biopsy is considered to be the reference standard for the final diagnosis and staging of HF [8, 9]. However, a liver biopsy has several recognized drawbacks: certain invasiveness,

high cost, sampling error, observation variations, poor repeatability, and so on [5, 9-11]. Therefore, it is not a suitable method to dynamically monitor and screen all patients with chronic liver diseases.

Magnetic resonance imaging (MRI), a noninvasive and promising technique for the evaluation of HF, has been increasingly adopted. Multiple b-value DWI as a non-contrast method has become a burning field of research in the assessment and staging of liver disease. In previously published reports [1, 8, 12] on HF, mono- and bi-exponential models of intravoxel incoherent motion (IVIM) have been proposed in HF. The bi-exponential model could describe the admixture of multiple exponential signal decays more closely than the mono-exponential model

and offered a possible unique insight into hepatic disease [13]. However, the bi-exponential model may oversimplify the movement of tissue water molecules in reality, and it is possibly more realistic to present a larger number (>2) of intravoxel proton pools using a continuous distribution of diffusion coefficients [14].

To present an alternative method to the bi-exponential model, Bennett *et al.* [14, 15] first introduced the stretched-exponential model, also referred to as the Kohlrausch decay function. The stretched-exponential model was used to present the IVIM diffusion signal and monitor the deviation from the mono-exponential model caused by pseudo-perfusion effects. The model perhaps overcame the difficulty of making a hypothesis about the amount of intravoxel proton pools utilizing distributed diffusion coefficients (DDC) in biological tissue. In a previous study, a stretched-exponential model was utilized to characterize the degree of intravoxel heterogeneity influencing diffusion-related MRI signal attenuation and has shown potential use for brain tumors [14, 16]. This paper will assess and compare the stretched-exponential model with the mono-exponential model in diagnosing and staging HF in patients, few articles have reported on this topic [17].

The purpose of this study was to calculate the parameters (DDC, α) of the stretched-exponential model using multi-b value DWI and evaluate whether these parameters could detect and stage HF in patients with chronic liver diseases with a better diagnostic performance than the parameter (ADC_{st}) of mono-exponential model.

Methods

Study population

The prospective study was approved by the institutional review board at the People's Hospital of Zhengzhou University, and informed consent was obtained from all participants for the respective assessment of their clinical data and images. Among them, 30 patients who had chronic liver diseases were recruited consecutively for this study between October 2012 and June 2013. All of them had undergone conventional MRI and multiple b-value DWI. Of these 30 patients, 5 were excluded from the study because of no liver biopsy or poor images. After

these exclusions, 25 patients (22 males and 3 females; mean age: 43.7±1.2 years, age range: 25-73 years) included in our study were verified by liver biopsy. Among the 25 patients, 15 were with hepatitis B, 1 with hepatitis C, 1 with alcoholic hepatitis, 2 with nonalcoholic fatty liver disease, 2 with drug induced hepatitis, 1 with Budd-Chiari syndrome, and 3 with autoimmune hepatitis. The time interval between undergoing the MRI and liver biopsy was one month. Of these 25 patients, 9 had abdominal distension and 16 were asymptomatic. At the same time, 25 control subjects (15 males and 10 females, mean age: 38.9±1.3 years, age range: 25-57 years) who had no history of liver disease, alcohol abuse, hepatic malignancy, or liver dysfunction were included. All the control subjects without ultrasound-guided liver biopsy had undergone conventional MRI and multiple b-value DWI.

Magnetic resonance examination

All MRI was performed on a 3.0 T scanner (Discovery MR750, GE Medical System, Milwaukee, Wis.) with an 8-channel body phased-array coil (GE Medical Systems). All participants underwent a routine liver MRI, which consisted of an axial T1-weighted spin echo sequence (repetition time (msec)/echo time (msec), 180/2.1), an axial T2-weighted spin echo sequence (repetition time (msec)/echo time (msec), 4286/88.1), and a coronal T2-weighted spin echo sequence (repetition time (msec)/echo time (msec), 8571/88.8). Multiple b-value DW-MRI was performed by using a respiratory-triggered single-shot spin-echo planar sequence, parallel imaging technique (parallel imaging reduction factor of 2), and monopolar gradient in the axial plane. The multiple b-value DW-MRI used following parameters: a repetition time (msec)/echo time (msec) of 7000~12000/62, section thickness of 3 mm, gap of 1 mm, field of view of 360 × 324 mm, matrix of 160 × 192. Seven b values from 0 to 800 sec/mm² (0, 50, 100, 200, 400, 600 and 800 sec/mm², with one signal acquired for b = 0 sec/mm², two signals acquired for b = 50, 100, 200 sec/mm², four signals acquired for b = 400, 600 sec/mm², and six signals acquired for b = 600, 800 sec/mm²) were used for performing DWI in three diffusion directions. The total slices of DWI varied on the basis of the length of the liver. Generally,

Diffusion weighted imaging in hepatic fibrosis

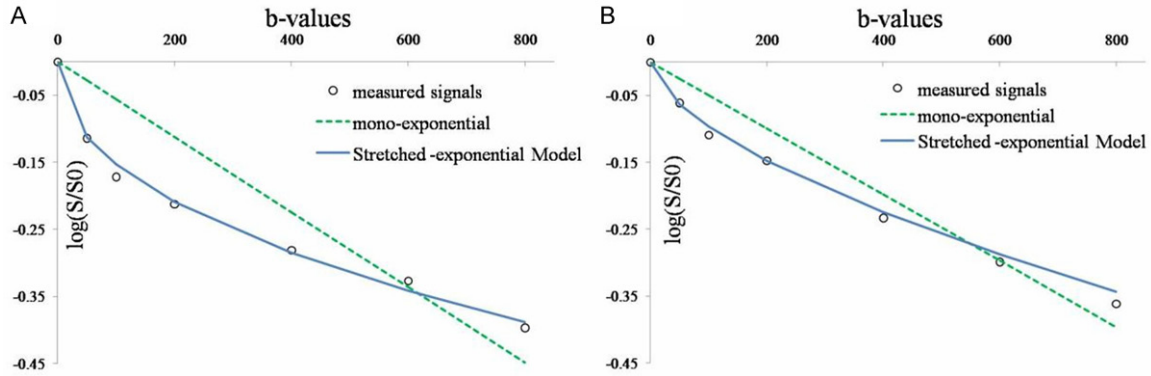


Figure 1. Semi-logarithmic plot of hepatic diffusion-related signal decay with respect to increasing b-values demonstrates improved fit of the raw data with a stretched-exponential model when compared to mono-exponential model. A. A 51-year-old female patient with no fibrosis (F0). B. A 38-year-old male patient with a history of hepatitis B with HF (F2).

Table 1. Distribution of Various Stages of Fibrosis and Grades of Histological activity

Fibrosis Stage	Histological Activity Grade				Total
	No (A0)	Mild (A1)	Moderate (A2)	Severe (A3)	
No fibrosis (F0)	10	0	0	0	10
Mild fibrosis (F1)	1	3	0	0	4
Moderate fibrosis (F2)	0	2	7	0	9
Advanced fibrosis (F3)	0	1	6	4	11
Cirrhosis fibrosis (F4)	0	0	0	1	1
Total	11	6	13	5	35

Note: F0 group includes 10 patients who were assumed to have healthy livers. The 10 patients without a histopathologic diagnosis with no evidence or history of liver disease, alcohol abuse, hepatic malignancy, or liver function test abnormalities were assumed to be fibrosis stage F0 and histological activity A0 in our study.

approximately 40 slices were obtained when performing multi-b value DWI.

Post-processing and image analysis

DWI processing and analysis was carried out on an Advantage Workstation 4.5 (GE Medical Systems). Two experienced radiologists (with 10 years of experience performing abdominal MRI) manually drew the regions of interest (ROIs) in the diffusion weighted image series (ADCst, DDC, α maps) for all b value. ROIs (150 mm²) [18] were placed in the right lobe to avoid large vessels, bile ducts, and focal hepatic lesions. Each ROI was measured 3 times, separately. After obtaining three ROI values, the average value was used for each patient. All the ROIs were drawn by two radiologists in consensus.

The ADCst was calculated using the mono-exponential model for all 8 b-values and fitted to the following equation: $S_b/S_0 = \exp(-bADC)$ [1]. Where S_b represents the signal intensity at a given diffusion weighting b, S_0 is the signal intensity without any diffusion weighting, and -b represents the diffusion sensitizing factor. ADC represents an apparent diffusion coefficient.

DDC and α were calculated using the stretched-exponential model which employed the following equation: $S_b/S_0 = \exp(-bDDC)^\alpha$ [2]. Where α , between 0 and 1, is the intravoxel water diffusion heterogeneity; the index DDC, the distributed diffusion coefficient, is the mean intravoxel diffusion rate.

In our work, we applied the least squares fit for a linear fitting with the mono-exponential model and the Levenberg-Marquardt fit for a nonlinear fitting with the stretched-exponential model. These were commonly used by fitting algorithms in previous studies (Figure 1A and 1B) [16, 19].

Liver histopathology

In our study, the METAVIR scoring system was used to semi-quantitatively evaluate the stage of fibrosis and histological activity [11, 20-22]. Fibrosis was staged on a scale of 0 to 4 as follows: F0, no fibrosis; F1, portal fibrosis without septa formation; F2, portal fibrosis with rare septa formation; F3, numerous septa formation without cirrhosis; F4, cirrhosis [23]. Histological activity was scored as follows: no activity (A0);

Diffusion weighted imaging in hepatic fibrosis

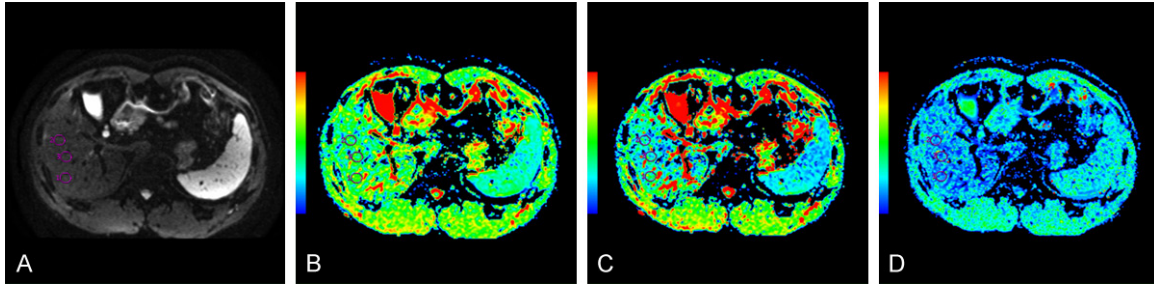


Figure 2. Characterization of a 51-year-old female patient with no fibrosis (F0). A. Multiple b-value DWI map of F0. B. The ADCst map shows the ADCst value was $1.29 \times 10^{-3} \text{ mm}^2/\text{s}$. C. The DDC map shows the DDC value was $0.973 \times 10^{-3} \text{ mm}^2/\text{s}$. D. The α map shows the α value was 0.447.

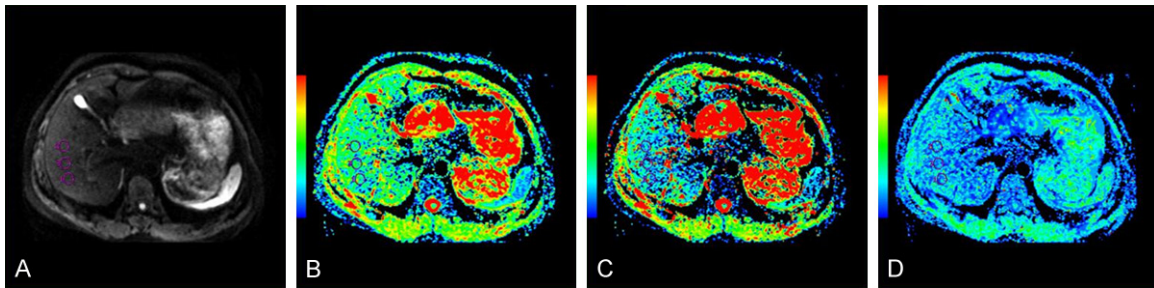


Figure 3. Characterization of a 38-year-old male patient with a history of hepatitis B with HF (F2). A. Multiple b-value DWI map of F2. B. The ADCst map shows decreased value ($1.14 \times 10^{-3} \text{ mm}^2/\text{s}$). C. The DDC map shows decreased value ($0.849 \times 10^{-3} \text{ mm}^2/\text{s}$). D. The α map shows increased value (0.610).

mild activity (A1); moderate activity (A2); and severe activity (A3). In the work, the fibrosis stage was verified by pathology of ultrasound-guided 18-gauge core liver biopsy. The liver biopsy specimen was taken from the right posterior lobe of the liver. Two experienced pathologists (with 15 years and 6 years of experience in abdominal diagnosis, respectively) blinded to all patients clinical and MRI data reviewed each of the specimens independently and provided METAVIR scores in consensus. Ten patients with healthy livers in control group were regarded as fibrosis stage F0 [2, 8].

Statistical analysis

All analyses were performed with SPSS statistical software (version 17.0; SPSS, Chicago, IL). A P -value <0.05 was considered to indicate a significant difference.

A series of paired sample t -tests were used to compare the ADCst, DDC and α values of this study group with the control group. Independent sample t -tests were also adopted to compare the ADCst, DDC and α of fibrosis stage 0 with stage 1-4, fibrosis stage 0-1 with stage 2-4 and

fibrosis stage 0-2 with stage 3-4 in this study group.

Pearson's correlation coefficient was used to assess the correlation between ADCst and DDC values of fibrosis groups. Pearson's correlation coefficient was also conducted to evaluate the correlation of all parameter (ADCst, DDC, α) values with stages of HF. Correlation coefficients were categorized by absolute value as follows: very weak to negligible correlation, 0.0-0.2; weak correlation, 0.2-0.4; moderate correlation, 0.4-0.7; strong correlation, 0.7-0.9; very strong correlation, 0.9-1.0 [24].

In the end, the area under the Receiver Operating Characteristic (ROC) curve was used to evaluate the performance of ADCst, DDC and α in discriminating fibrosis stage 1 or greater, stage 2 or greater, and stage 3 or greater. We obtained the maximum of the sum of sensitivity and specificity by choosing optimal cutoff values for multiple b-value DWI.

Results

The fibrosis stages and histological activity grades of the 35 cases (including 25 patients

Table 2. Comparison of the parameters between the study and control groups

Parameters	Study Group	Control Group	P
	(n = 25) Values	(n = 25) Values	
	Mean ± SD	Mean ± SD	
ADCst*	1.14±0.16	1.36±0.16	0.000
DDC*	0.82±0.09	1.04±0.13	0.000
α	0.55±0.04	0.57±0.04	0.047

* = ($\times 10^{-3}$ mm²/s).

Table 3. Correlation coefficients between parameters and fibrosis stages in the study group

Parameters	r	p
ADCst	-0.591	0.000
DDC	-0.786	0.000
α	-0.312	0.068

with chronic liver diseases and 10 patients with healthy livers in control group) are presented in **Table 1**. Among the 35 patients, the fibrosis stage distributions are as follows: F0 group included 10 patients who were assumed to have healthy livers and no histological activity [2, 8] (**Figures 1A, 2A-D**), F1 group included 4 patients who had no (1 case) or mild histological activity (3 cases). F2 group included 9 patients who had mild (2 cases) or moderate histological activity (7 cases) (**Figures 1B, 3A-D**). F3 group included 11 patients who had mild to severe histological activity. F4 group included only 1 patient who had severe histological activity.

A paired sample t-test was used for the study and control groups. As shown in **Table 2**, the mean ADCst, DDC and α values of the liver in the study group were different from the corresponding parameters in the control group, respectively (all P<0.05).

Pearson's correlation coefficient was used to evaluate the correlation of the values (ADCst, DDC and α) with fibrosis stages. The results are shown in **Table 3**. Both the mean ADCst and DDC values show a negative correlation with the fibrosis stages ($r = -0.591$ and -0.786 , all P<0.001), i.e. the ADCst and DDC values decrease with an increase of the stage of the fibrosis. However, α values show no significant correlation with the HF stages (P>0.05). Pearson's correlation coefficient was also adopted

to assess the correlation between ADCst and DDC. There was a moderate positive correlation between ADCst and DDC ($r = 0.596$, P<0.001).

As shown in **Table 4**, independent sample t-tests were used to compare fibrosis stage 0 with stage 1-4 (F0 vs. F1-F4), fibrosis stage 0-1 with stage 2-4 (F0-F1 vs. F2-F4), fibrosis stage 0-2 with stage 3-4 (F0-F2 vs. F3-F4) in the ADCst, DDC, and α values. We found that groups F0, F0-F1 and F0-F2 of HF were significantly different from groups F1-F4, F2-F4 and F3-F4 in the mean values of ADCst or DDC, respectively (all P<0.05). The α values of groups F0, F0-F1 and F0-F2 showed no significant difference from groups F1-F4, F2-F4 and F3-F4, respectively (all P>0.05).

According to the ROC analysis (**Figure 4A-C**), the areas under the curves (AUCs) of the DDC, ADC and α for differentiating F0 from F1-4 were 0.912, 0.948, and 0.694, respectively. The AUCs of DDC, ADC and α for differentiating F1 from F2-4 were 0.850, 0.903, and 0.730, respectively. The AUCs of DDC, ADC and α for differentiating F2 from F3-4 were 0.741, 0.879, and 0.679, respectively. The DDC and ADC were significant parameters for differentiating F0 from F1-4, F1 from F2-4, F2 from F3-4 (all P<0.05, **Table 5**). Although α was a significant parameter for differentiating F1 from F2-4 (P<0.05), it was not a significant parameter for differentiating F0 from F1-4, F2 from F3-4 (all P>0.05, **Table 5**). Based on ROC analysis (**Figure 4A-C**), the optimal cutoff values, sensitivity, and specificity are summarized in **Table 5**.

Discussion

In this study, we quantitatively evaluated HF in patients with chronic liver diseases using the stretched-exponential and mono-exponential models. The results showed that the DDC from the stretched-exponential model provided greater diagnostic accuracy in staging HF than the ADCst from the mono-exponential model when histopathology was used as the reference standard. Therefore, DDC may serve as an optimal diffusion parameter for diagnosis and staging of HF.

In our study, the results showed that ADCst, DDC of the fibrotic livers in the study group were significantly different from the corre-

Diffusion weighted imaging in hepatic fibrosis

Table 4. Comparison of mean values between fibrosis stages

Parameter	F0 and F1-F4 Values		F0-F1 and F2-F4 Values		F0-F2 and F3-F4 Values	
	Mean ± SD		Mean ± SD		Mean ± SD	
ADCst*	1.41±0.11	1.14±0.16	1.34±0.20	1.13±0.13	1.27±0.20	1.12±0.14
DDC*	1.03±0.10	0.82±0.09	0.99±0.12	0.81±0.09	0.94±0.12	0.77±0.08
α	0.57±0.06	0.55±0.04	0.57±0.05	0.54±0.04	0.56±0.04	0.54±0.05
P value						
ADCst*	0.000		0.003		0.014	
DDC*	0.000		0.000		0.000	
α	0.248		0.103		0.116	

* = ($\times 10^{-3}$ mm²/s).

sponding parameters of the normal livers in the control group. Since HF is a nonspecific response to chronic liver diseases that results in excessive synthesis and deposition of extracellular matrix (ECM), particularly collagen fibers, in which the protons are less ample and tightly bound [25, 26] the water molecular diffusion would be restricted in fibrotic liver because of collagen fibers existing in the distorted lobular tissue. As a consequence, ADCst values decrease in a fibrotic liver when compared with a normal liver. The DDC can be supposed as a weighted sum over a continuous distribution of ADCst that is comprised of the multi-exponential decay properties. Therefore, DDC demonstrates a theoretically more accurate description of diffusion in the present of multi-exponential decay and decrease in the fibrotic liver when compared with a normal liver [14, 16]. In pioneering studies, Patel *et al.* [27] and Luciani *et al.* [28] all found that the mean ADC values in the fibrotic and cirrhotic liver groups were lower than the values in the healthy liver group with multiple b-values (1.41×10^{-3} mm²/s vs. 1.73×10^{-3} mm²/s [27]; 1.23×10^{-3} mm²/s vs. 1.39×10^{-3} mm²/s [28]). So far, only Anderson *et al.* has reported on the stretched-exponential model in evaluating murine's HF with high b values [17]; there is no report on the stretched-exponential model in evaluating human HF. As shown in this study, we also found that both the mean ADCst and DDC values of fibrotic liver in the study group were significantly lower than the values of those in the normal livers in the control group (1.14×10^{-3} mm²/s vs. 1.36×10^{-3} mm²/s; 0.82×10^{-3} mm²/s vs. 1.04×10^{-3} mm²/s). Interestingly, our results showed that the mean α value of the fibrotic liver in the study group was different from the normal liver and was slightly lower

than the normal liver, although there is no clear evidence to prove that a fibrotic liver may exhibit more intravoxel diffusion heterogeneity than a normal liver.

With increasing HF stages, the accumulation of the extracellular matrix (including collagen fibers and proteins *etc.*) would gradually increase. Thereafter, the water molecular diffusion would be obviously restricted with the increasing fibrosis stage. The ADCst and DDC values would decrease with the increase of the HF stage. In our work, the DDC demonstrated a strong negative correlation with the HF stages ($r = -0.786$), while ADCst demonstrated a moderate correlation with the HF stages ($r = -0.579$). The above-mentioned results were similar to previous findings [17]. In our work, we also found that group fibrosis stages (*i.e.*, stage 0, stage 0-1 and stage 0-2) were significantly different from the group fibrosis stage 1-4, stage 2-4 and stage 3-4, in the mean values of ADCst or DDC, respectively (all $P < 0.05$).

The α values have no significant correlation with the HF stages. The parameter α, which characterizes the deviation from mono-exponential decay in the stretched-exponential models, is supposed to represent an increase in intravoxel heterogeneity. Nevertheless, the biological explanation of the increase in intravoxel heterogeneity has not yet been defined so far. Previous studies showed the increase in intravoxel heterogeneity in malignant tumors and reported the finding is a sign of brain tumor invasion [16, 17, 29-32]. In the study, our result demonstrated a lack correlation between HF stages and the α value. We also found that the fibrosis stage 0, stage 0-1 and stage 0-2 had no significant differences in α values when com-

Diffusion weighted imaging in hepatic fibrosis

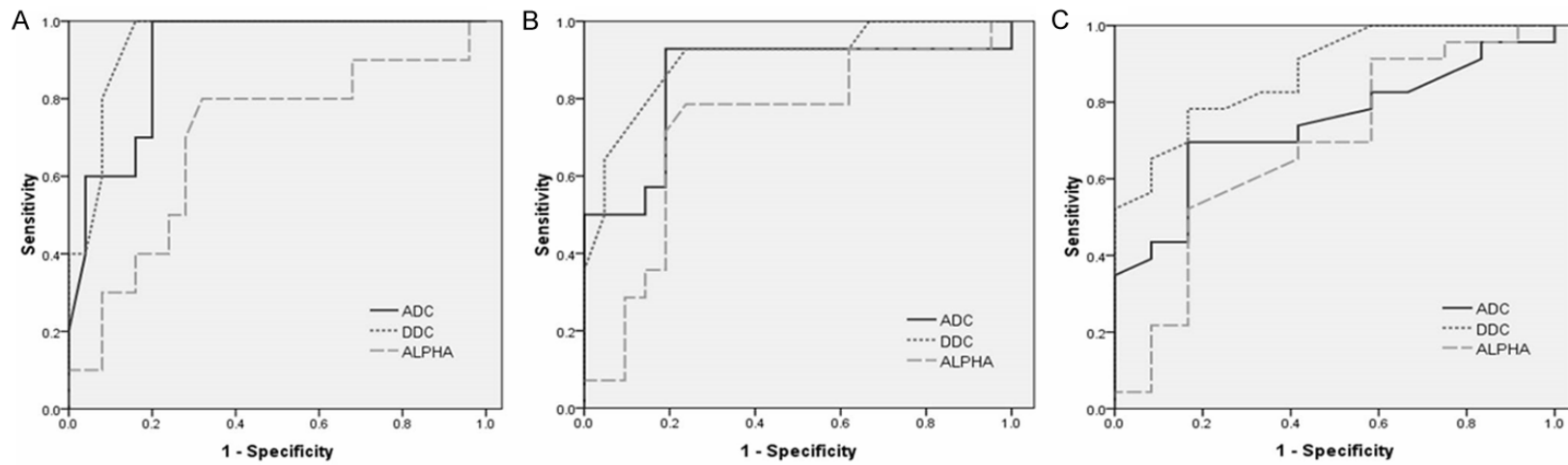


Figure 4. Analysis of ADCst, DDC and α in distinguishing stages of HF by ROC curve. A. ROC analysis for ADCst, DDC and α to distinguish HF stage 1 or greater (F0 vs. F1-F4). B. ROC analysis for ADCst, DDC and α to distinguish HF stage 2 or greater (F0-F1 vs. F2-F4). C. ROC analysis for ADCst, DDC and α to distinguish HF stage 3 or greater (F0-F2 vs. F3-F4).

Table 5. Comparison of ADCst, DDC and α in predicting and staging HF according to optimal cutoff values

Parameter	F0/ F1-F4	F0-F1/ F2-F4	F0-F2/ F3-F4
ADCst*			
Cutoff value	1.275	1.215	1.205
AUC	0.912	0.850	0.741
Sensitivity (%)	100	92.9	69.6
Specificity (%)	80	81	83.3
P	0.000	0.001	0.021
DDC*			
Cutoff value	0.905	0.855	0.845
AUC	0.948	0.903	0.879
Sensitivity (%)	100	92.9	78.3
Specificity (%)	84	76.2	83.3
P	0.000	0.000	0.000
α			
Cutoff value	0.562	0.562	0.564
AUC	0.694	0.730	0.679
Sensitivity (%)	80	78.6	52.2
Specificity (%)	68	76.2	83.3
P	0.077	0.023	0.085

* = ($\times 10^{-3}$ mm²/s).

pared with the fibrosis stage 1-4, stage 2-4 and stage 3-4, respectively. Hence, no clear evidence of increasing stages of HF accompanied by an increase in intrvoxel heterogeneity were detected using the stretched-exponential model [17].

According to the ROC analysis, the AUC values of ADCst for differentiating group F0 from F1-F4, F0-F1 from F2-F4, F0-F2 from F3-F4 were 0.912, 0.850, 0.741, respectively (all $P < 0.05$; **Table 5**). The AUC values of DDC for differentiating F0 from F1-F4, F0-F1 from F2-F4, F0-F2 from F3-F4 were 0.948, 0.903, 0.879, respectively (all $P < 0.05$; **Table 5**). The AUC values of α for differentiating F0-F1 from F2-F4 were 0.730 ($P < 0.05$) and was lower than that of DDC and ADCst. However, α was not a significant parameter for differentiating F0 from F1-F4, F0-F2 from F3-F4 ($P = 0.077, 0.085$, respectively; **Table 5**). The results indicate that the ADCst and DDC were significant parameters for differentiating the above-mentioned groups (all the AUC values between 0.7 and 0.9). Moreover, our results demonstrated for the first time that DDC showed a slightly better diagnostic ability than ADCst for differentiating the above-mentioned groups. Therefore, we

could consider that DDC demonstrates a more accurate description of diffusion in the presence of multi-exponential models [14, 15, 30, 32]. It is generally accepted that patients without HF or with early HF (F0-F1) have a lower risk for hepatocellular carcinoma or liver failure, while significant HF (F2-F4) is a prediction of future hepatic cirrhosis and is also an indicant for therapy in hepatitis C patients [33]. Previous studies [8, 34, 35] have reported that HF stage 0-2 is described as mild-moderate fibrosis, and its progression can be prevented by clinical intervention and treatment. However, it is difficult to reverse HF stage 3-4 which is described as advanced HF. Hence, we believe that DDC may have important greater clinical implications for guiding clinical treatment and assessing the effect of the therapy for patients with chronic liver diseases than ADCst.

A moderate positive correlation of ADCst with the potentially more accurate DDC values of the HF was discovered in the study ($r = 0.596$). This finding could be explained by the stretched-exponential model. Reviewing Eqs. (1) ($S_v/S_0 = \exp(-b \times ADC)$) and Eqs. (2) ($S_v/S_0 = \exp(-b \times DDC^a)$), we could obtain the following equation: $ADC = b^{a-1} \times DDC^a$. (3) when $b \times DDC = 1$ (regardless of a value) or when $a = 1$ (regardless of b-value or DDC), $DDC \approx ADC$. If $a < 1$, and $b \times DDC > 1$, DDC will be higher than ADC. In contrast, if $a < 1$, and $b \times DDC < 1$, DDC will be lower than ADC. While the degree of agreement between ADCst and DDC in the study is lower than the previous studies [30, 36] which found a strong positive correlation ($R = 0.9716, 0.99, 0.98, 0.99$, all $P < 0.05$) between ADCs and DDCs of high-grade gliomas, prostate cancer, normal peripheral zone and normal central gland tissues. At present, this finding could not yet be clearly explained. For the moment it is still indistinct if, and to what extent, DDCs and ADCs of other diseases agree. Hence, this issue remains conjectural and further study is needed.

There are a few limitations to the study. First, the number of subjects was small, although prior studies have had similar small numbers of cases [37]. We plan on performing a study with a large number of patients in each fibrosis stage. Second, we didn't analyze fat or iron deposition in HF and didn't know whether they might affect the ADCst, DDC, and α values. Further work will be conducted to explore these possibilities.

In conclusion, ADCst and DDC showed a significant correlation with significant HF. Furthermore, DDC showed a higher diagnostic performance than ADCst for discriminating HF stages. Therefore, our study demonstrates the stretched-exponential and mono-exponential model of multiple-b value DWI may provide a noninvasive quantitative method of assessing and staging HF. We further believe the parameters (DDC, ADCst) could be used as an alternative marker for HF, offering help in the clinical diagnosis of HF, monitoring its progression, guiding therapy and assessing the effect of treatment.

Acknowledgements

This work was supported by the National Natural Science Foundation of China (Grant Nos. 81271534 and 31470047).

Disclosure of conflict of interest

None.

Address correspondence to: Dr. Dapeng Shi, Department of Radiology, The People's Hospital of Zhengzhou University & Henan Provincial People's Hospital, Zhengzhou 450003, Henan, China. Tel: +86 37165580930; E-mail: shidapengsyy@126.com

References

- [1] Chow AM, Gao DS, Fan SJ, Qiao Z, Lee FY, Yang J, Man K, Wu EX. Liver fibrosis: An intravoxel incoherent motion (IVIM) study. *J Magn Reson Imaging* 2012; 36: 159-167.
- [2] Watanabe H, Kanematsu M, Goshima S, Kondo H, Onozuka M, Moriyama N, Bae KT. Staging Hepatic Fibrosis: Comparison of Gad-oxetate Disodium-enhanced and Diffusion-weighted MR Imaging-Preliminary Observations. *Radiology* 2011; 259: 142-150.
- [3] Shim JH, Yu JS, Chung JJ, Kim JH, Kim KW. Segmental Difference of the Hepatic Fibrosis from Chronic Viral Hepatitis due to Hepatitis B versus C Virus Infection: Comparison Using Dual Contrast Material-Enhanced MRI. *Korean J Radiol* 2011; 12: 431-438.
- [4] Wang Y, Ganger DR, Levitsky J, Sternick LA, McCarthy RJ, Chen ZE, Fasanati CW, Bolster B, Shah S, Zuehlsdorff S, Omary RA, Ehman RL, Miller FH. Assessment of chronic hepatitis and fibrosis: comparison of MR elastography and diffusion-weighted imaging. *AJR Am J Roentgenol* 2011; 196: 553-561.
- [5] Yoon JH, Lee JM, Woo HS, Yu MH, Joo I, Lee ES, Sohn JY, Lee KB, Han JK, Choi BI. Staging of Hepatic Fibrosis: Comparison of Magnetic Resonance Elastography and Shear Wave Elastography in the Same Individuals. *Korean J Radiol* 2013; 14: 202-212.
- [6] Arthur MJ. Reversibility of liver fibrosis and cirrhosis following treatment for hepatitis C. *Gastroenterology* 2002; 122: 1525-1528.
- [7] Lim YS, Kim WR. The global impact of hepatic fibrosis and end-stage liver disease. *Clin Liver Dis* 2008; 12: 733-746.
- [8] Chen C, Wang B, Shi D, Fu F, Zhang J, Wen Z, Zhu S, Xu J, Lin Q, Li J, Dou S. Initial study of biexponential model of intravoxel incoherent motion magnetic resonance imaging in evaluation of the liver fibrosis. *Chin Med J* 2014; 127: 3082-3087.
- [9] Lee JE, Lee JM, Lee KB, Yoon JH, Shin CI, Han JK, Choi BI. Noninvasive Assessment of Hepatic Fibrosis in Patients with Chronic Hepatitis B Viral Infection Using Magnetic Resonance Elastography. *Korean J Radiol* 2014; 15: 210-217.
- [10] Bonekamp S, Torbenson MS, Kamel IR. Diffusion-weighted Magnetic Resonance Imaging for the Staging of Liver Fibrosis. *J Clin Gastroenterol* 2011; 45: 885-892.
- [11] Fujimoto K, Tonan T, Azuma S, Kage M, Nakashima O, Johkoh T, Hayabuchi N, Okuda K, Kawaguchi T, Sata M, Qayyum A. Evaluation of the Mean and Entropy of Apparent Diffusion Coefficient Values in Chronic Hepatitis C: Correlation with Pathologic Fibrosis Stage and Inflammatory Activity Grade. *Radiology* 2011; 258: 739-748.
- [12] Ichikawa S, Motosugi U, Morisaka H, Sano K, Ichikawa T, Enomoto N, Matsuda M, Fujii H, Onishi H. MRI-based staging of hepatic fibrosis: Comparison of intravoxel incoherent motion diffusion-weighted imaging with magnetic resonance elastography. *J Magn Reson Imaging* 2015; 42: 204-210.
- [13] Maier SE, Bogner P, Bajzik G, Mamata H, Mamata Y, Repa I, Jolesz FA, Mulkern RV. Normal brain and brain tumor: multicomponent apparent diffusion coefficient line scan imaging. *Radiol* 2001; 219: 842-849.
- [14] Bennett KM, Schmainda KM, Bennett RT, Rowe DB, Lu H, Hyde JS. Characterization of continuously distributed cortical water diffusion rates with a stretched-exponential model. *Magn Reson Med* 2003; 50: 727-734.
- [15] Bennett KM, Hyde JS, Schmainda KM. Water diffusion heterogeneity index in the human brain is insensitive to the orientation of applied magnetic field gradients. *Magn Reson Med* 2006; 56: 235-239.

Diffusion weighted imaging in hepatic fibrosis

- [16] Kwee TC, Galbán CJ, Tsien C, Junck L, Sundgren PC, Ivancevic MK, Johnson TD, Meyer CR, Rehemtulla A, Ross BD, Chenevert TL. Intravoxel water diffusion heterogeneity imaging of human high-grade gliomas. *NMR Biomed* 2010; 23: 179-187.
- [17] Anderson SW, Barry B, Soto J, Ozonoff A, O'Brien M, Jara H. Characterizing Non-Gaussian, High b-value Diffusion in Liver Fibrosis: Stretched Exponential and Diffusional Kurtosis Modeling. *J Magn Reson Imaging* 2014; 39: 827-834.
- [18] Filipe JP, Curvo-Semedo L, Casalta-Lopes J, Marques MC, Caseiro-Alves F. Diffusion-weighted imaging of the liver: usefulness of ADC values in the differential diagnosis of focal lesions and effect of ROI methods on ADC measurements. *Magn Reson Mater Phy* 2013; 26: 303-312.
- [19] Bai Y, Lin Y, Tian J, Shi D, Cheng J, Haacke EM, Hong X, Ma B, Zhou J, Wang M. Grading of Gliomas by Using Monoexponential, Biexponential, and Stretched Exponential Diffusion-weighted MR Imaging and Diffusion Kurtosis MR Imaging. *Radiology* 2016; 278: 496-504.
- [20] Ishak K, Baptista A, Bianchi L. Histological grading and staging of chronic hepatitis. *J Hepatol* 1995; 22: 696-699.
- [21] Mallet V, Gilgenkrantz H, Serpaggi J, Verkarre V, Vallet-Pichard A, Fontaine H, Pol S. Brief communication: the relationship of regression of cirrhosis to outcome in chronic hepatitis C. *Ann Intern Med* 2008; 149: 399-403.
- [22] Taouli B, Tolia AJ, Losada M, Babb JS, Chan ES, Bannan MA, Tobias H. Diffusion weighted MRI for quantification of liver fibrosis: preliminary experience. *AJR Am J Roentgenol* 2007; 189: 799-806.
- [23] Bedossa P, Poynard T; The French METAVIR Cooperative Study Group. An algorithm for grading activity in chronic hepatitis C. *Hepatology* 1996; 24: 289-293.
- [24] Karlik SJ. Exploring and summarizing radiologic data. *AJR Am J Roentgenol* 2003; 180: 47-54.
- [25] Friedman SL. Molecular regulation of hepatic fibrosis, an integrated cellular response to tissue injury. *J Biol Chem* 2000; 275: 2247-2250.
- [26] Wynn TA. Cellular and molecular mechanisms of fibrosis. *J Pathol* 2008; 214: 199-210.
- [27] Patel J, Sigmund EE, Rusinek H, Oei M, Babb JS, Taouli B. Diagnosis of cirrhosis with intravoxel incoherent motion diffusion MRI and dynamic contrast-enhanced MRI alone and in combination: preliminary experience. *J Magn Reson Imaging* 2010; 31: 589-600.
- [28] Luciani A, Vignaud A, Cavet M, Nhieu JT, Mallat A, Ruel L, Laurent A, Deux JF, Brugieres P, Rahmouni A. Liver cirrhosis: intravoxel incoherent motion MR imaging-pilot study. *Radiology* 2008; 249: 891-899.
- [29] Hoff BA, Chenevert TL, Bhojani MS, Kwee TC, Rehemtulla A, Le Bihan D, Ross BD, Galbán CJ. Assessment of multiexponential diffusion features as MRI cancer therapy response metrics. *Magn Reson Med* 2010; 64: 1499-1509.
- [30] Kwee TC, Galbán CJ, Tsien C, Junck L, Sundgren PC, Ivancevic MK, Johnson TD, Meyer CR, Rehemtulla A, Ross BD, Chenevert TL. Comparison of apparent diffusion coefficients and distributed diffusion coefficients in high grade gliomas. *J Magn Reson Imaging* 2010; 31: 531-537.
- [31] Palombo M, Gabrielli A, De Santis S, Capuani S. The γ parameter of the stretched-exponential model is influenced by internal gradients: validation in phantoms. *J Magn Reson* 2012; 216: 28-36.
- [32] Bennett KM, Hyde JS, Rand SD, Bennett R, Krouwer HG, Rebro KJ, Schmainda KM. Intravoxel distribution of DWI decay rates reveals C6 glioma invasion in rat brain. *Magn Reson Med* 2004; 52: 994-1004.
- [33] Ghany MG, Strader DB, Thomas DL, Seeff LB. Diagnosis, management, and treatment of hepatitis C: an update. *Hepatology* 2009; 49: 1335-1374.
- [34] Afdhal NH. Diagnosing fibrosis in hepatitis C: is the pendulum swinging from biopsy to blood tests? *Hepatology* 2003; 37: 972-974.
- [35] Kim AI, Saab S. Treatment of hepatitis C. *Am J Med* 2005; 118: 808-815.
- [36] Liu X, Zhou L, Peng W, Wang H, Zhang Y. Comparison of stretched-Exponential and monoexponential model diffusion-Weighted imaging in prostate cancer and normal tissues. *J Magn Reson Imaging* 2015; 42: 1078-85.
- [37] Dyvorne HA, Galea N, Nevers T, Fiel MI, Carpenter D, Wong E, Orton M, de Oliveira A, Feiweier T, Vachon ML, Babb JS, Taouli B. Diffusion-weighted Imaging of the Liver with Multiple b Values: Effect of Diffusion Gradient Polarity and Breathing Acquisition on Image Quality and Intravoxel Incoherent Motion Parameters-A Pilot Study. *Radiology* 2013; 266: 920-929.